

# A Novel Parallel 2-DOF Spherical Mechanism with One-to-One Input-Output Mapping

WEIMIN LI, JIANGUANG SUN, JIANJUN ZHANG  
School of Mechanical Engineering,  
Hebei University of Technology,  
Tianjin 300130, CHINA

KAI HE, R. DU  
Institute of Precision Engineering,  
The Chinese University of Hong Kong,  
Shatin, N. T., Hong Kong, CHINA

*Abstract:* - This paper presents a novel decoupled parallel 2-DOF spherical mechanism. First, the design idea is introduced based on a general 2-DOF spherical mechanism. Next, following the discussions of some practical types of flat pairs, the new mechanism is given. Besides, the new mechanism uses a planar parallelogram to replace the prismatic pair to achieve the simple kinematics of one-to-one input-output mapping with minimum requirement on actuators. The workspace of the mechanism is also analyzed, in which the effect of friction circle of the revolute joint is considered.

*Key-Words:* - Decoupled, Parallel, Spherical mechanism, One-to-one, Input-output mapping, Workspace

## 1 Introduction

Since the variable-length-strut octahedral hexapod with six degrees of freedom (DOFs) was introduced by Gough for tire detecting device [1] and afterwards by Stewart for flight simulator [2], parallel mechanisms have found many practical applications such as heavy loading platforms, special machines with extraordinary kinematical and dynamical performance, precise positioning manipulators and etc. A typical parallel mechanism consists of a moving platform, a fixed base, and several kinematical chains (also called the legs) which connecting the moving platform to its base. Only some kinematical pairs are actuated, whose number usually equals to the number of DOF that the platform possesses with respect to the base. Frequently, the number of legs equals to that of DOF. This makes it possible to actuate only one pair per leg, allowing all motors to be mounted close to the base. Such mechanisms show desirable characteristics, such as large payload and weight ratio, large stiffness, low inertia, and high dynamic performance. Though, compared with serial manipulators, its disadvantages include lower dexterity, smaller workspace, and more seriously,

singularity, by which the functioning of the mechanism is disruptive.

In the past two decades, parallel mechanisms with fewer than 6-DOF have attracted much attentions. These mechanisms have the advantages of simpler architecture and lower manufacturing cost. In particular, parallel spherical mechanisms allow the platform to rotate around a fixed point and may be used to orient an object. The object may be a telescope, an antenna, a solar panel, a camera, a tool, the end-effector of a robot, a human or humanoid artificial limb, and etc.

Spherical mechanisms may take various configurations. Some of them use spherical architectures, in which only revolute joints are used and their axes intersect at a common center point; as a result, the moving links constitute paths located on concentric spherical surfaces [3-7]. Others use dissimilar architectures, in which the links do not need to move along any spherical surfaces. They only require that the constraints imposed by the legs on the platform provide a fixed center of rotation. This kind of design can achieve the benefit of being able to choose leg topologies in a large range [8-13]. Another possible scheme uses an additional spherical

pair which physically connects the platform to the center of rotation, so the legs do not have to provide constraints which can give the platform a fixed center. As a result, the legs can be freely designed [14-17]. However, most of these configurations have coupled motion between the orientations of the moving platform. In fact, little research has been reported on the study of orientation decoupling [18, 19], while much more research concentrate on the translational motion decoupling [20-29].

This paper focuses on the decoupled synthesis of 2-DOF spherical mechanism. The interest for this case is justified by the fact that, in many applications, a 2-DOF orientation device is sufficient. A typical application is the positioning of solar panel. In order to facilitate the control (tracing the sun), a decoupled mechanism is highly desirable.

The paper presents a novel parallel 2-DOF spherical mechanism with one-to-one input-output mapping. A model of prototype is also presented to simulate the potential actual workspace of the mechanism and to show its considerable mobility capabilities. The rest of the paper is organized as follows. Section 2 presents a systematic study on the 2-DOF spherical mechanisms. Section 3 presents the new design. Section 4 is a study of the workspace of the new mechanism. Finally, Section 5 draws the conclusions.

## 2 A Study on the General Geometry of a 2-DOF Spherical Mechanism

For the convenience of the discussions, first, let us introduce three kinds of joints (or pairs) as shown in Figure 1. They are the revolute joint (R), the prismatic pair (P), and the planar pair or flat pair (F). They possess one revolute DOF, one translational DOF and three DOF (two translational and one revolute) respectively.

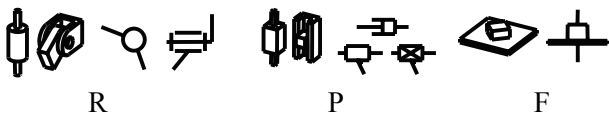


Fig.1: Definition of pairs or joints

Figure 2 illustrates the general geometry of a decoupled 2-DOF spherical mechanism. The moving platform is anchored to the base by two legs. A leg consists of two revolute joints,  $R_1$  and  $R_2$ , whose axes,  $z_1$  and  $z_2$ , intersect at point  $o$  and connect to each other perpendicularly to form a universal joint; so the value of  $\alpha$  is  $\pi/2$ . The other leg consists of a revolute joint,  $R_3$ , a flat pair,  $F$ , and a prismatic pair  $P$ , in

which the moving direction of  $P$  is perpendicular to the working plane of  $F$  and the axis of  $R_3$ . The revolute joints  $R_2$  and  $R_3$  are mounted on the moving platform in parallel. The prismatic pair  $P$  and the revolute joint  $R_1$  are assembled to the base, in which the moving direction of  $P$  is parallel to the axis of  $R_1$ .

Suppose that the input parameters,  $q_1$  and  $q_2$ , represent the positions of the revolute joint  $R_1$  and the prismatic pair  $P$ , which are driven by a rotary actuator and a linear actuator separately. The pose of the moving platform is defined by the Euler angles  $\theta_1$  and  $\theta_2$  of the platform. When the value of  $q_1$  changes and  $q_2$  holds the line, only  $\theta_1$  alters. On the other hand, when the value of  $q_2$  changes, only  $\theta_2$  changes. So,  $\theta_1$  and  $\theta_2$  are independently determined by  $q_1$  and  $q_2$  respectively, i.e., one output parameter only relates to one input parameter. In other words, the platform rotations around two axes are decoupled.

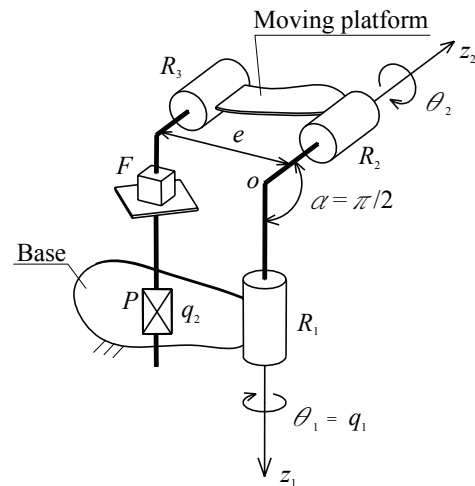


Fig.2: Illustration of a general spherical mechanism

Let  $e$  be the distance between the axes of  $R_2$  and  $R_3$ . Also, suppose that, when the moving platform is on the initial position, the axis of  $R_1$  is perpendicular to the plane consisting of the axes of  $R_2$  and  $R_3$ . Then the displacement relationships between input and output are:

$$\begin{cases} q_1 = \theta_1 \\ q_2 = e \cdot \sin \theta_2 \end{cases} \quad (1)$$

Taking the derivative of Equation (1), it follows that

$$\begin{bmatrix} \dot{q}_1 \\ \dot{q}_2 \end{bmatrix} = J^{-1} \begin{bmatrix} \dot{\theta}_1 \\ \dot{\theta}_2 \end{bmatrix} \quad (2)$$

where,

$$J = \begin{bmatrix} 1 & 0 \\ 0 & e \cdot \cos \theta_2 \end{bmatrix} \quad (3)$$

Furthermore, applying the principle of virtual work

to Equation (1), we get

$$\begin{bmatrix} f_1 \\ f_2 \end{bmatrix} = J^T \begin{bmatrix} T_1 \\ T_2 \end{bmatrix} \quad (4)$$

where,  $T_j$  is the output torque of the platform output,  $f_j$  is the input torque for  $R_1$  and the input force for  $P$ , and  $j = 1, 2$ .

Although this architecture is decoupled in motion, the input-output relationship for  $q_2 \rightarrow \theta_2$  through leg of  $PFR_3$  is nonlinear. Moreover, if  $\theta_2 \rightarrow \pm\pi/2$ , then, according to Equation (4), for a small output torque  $T_2$ , the input force will be  $f_2 \rightarrow \infty$ . For example, suppose  $e = 100$  mm and the output torque is  $T = 1$  N·m, then the input force  $f_2$  varies depending on the value of  $\theta_2$ , as shown in Figure 3. From the figure, it is seen that the driving force rises rapidly when  $|\theta_2| > 60^\circ$ . Clearly, this is not desirable.

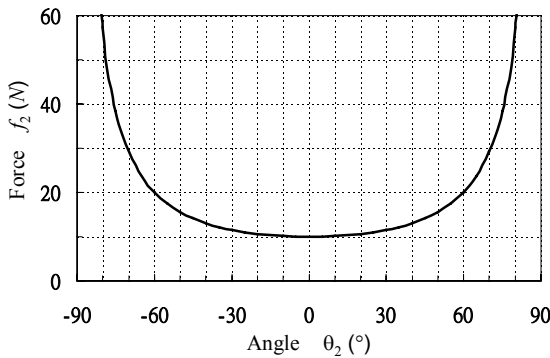
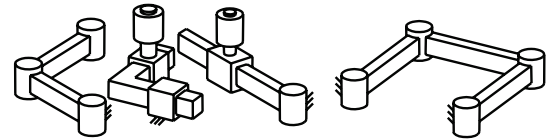


Fig.3: The input force required for constant torque output of  $T = 1$  N·m

To overcome the aforementioned shortcoming, an improved architecture which has the character of one-to-one input-output mapping is therefore proposed.

### 3 Improved Architecture with One-to-One Input-Output Mapping

The proposed new architecture is based on the fact that F-pair can be replaced by various other architectures, provided that they can offer the equivalent DOF. Also, it is possible to transform the P-pair into other mode to get the linear input-output relationship. Figure 4 shows the possible substitutes for F-pair and P-pair. Figure 4(a) shows three architectures, 3R, PPR and RPR that can replace F-pair; Figure 4(b) shows a planar parallelogram (4R) that can replace P-pair. Furthermore, compared with PPR and RPR, 3R is the most suitable substitution of F-pair since it is easy to manufacture.



(a) F-pair (3R, PPR, RPR) (b) P-pair (4R)  
Fig. 4: Substitute for F-pair and P-pair

Figure 5 shows the new architecture of the 2-DOF spherical mechanism developed from the one in Figure 2, in which the F-pair and the P-pair are replaced by 3R ( $R_4 - R_6$ ) and 4R ( $R_7 - R_{10}$ ) respectively. Note that the links  $\overline{R_7R_8}$  and  $\overline{R_9R_{10}}$  of the planar parallelogram are always parallel to the axis  $R_1$ . In this case, both inputs can be driven by rotary actuators. One actuator should be applied on  $R_1$ , and the other can be fixed on  $R_9$  or  $R_{10}$ . The reference point of the platform,  $P$ , will be used in workspace analysis.

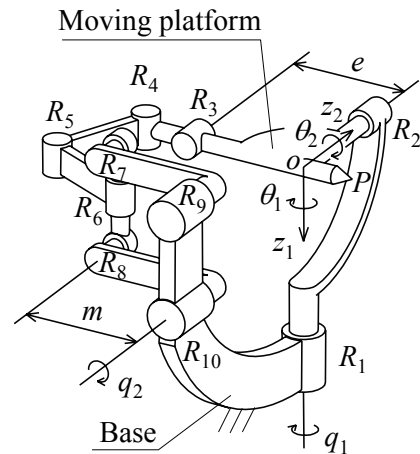


Fig. 5: The new architecture of 2-DOF spherical mechanism

Let us suppose that, at the initial position, the links of  $\overline{R_7R_9}$  and  $\overline{R_8R_{10}}$  of the planar parallelogram are parallel to  $\overline{oR_3}$  and perpendicular to the axis of  $R_1$ , and their length is  $m$ . Compared with the architecture in Figure 2, in the new architecture, the input related to  $\theta_2$  is based on the revolute input  $R_9$  or  $R_{10}$  (instead of the prismatic input  $P$ ). This difference can be mathematically expressed as that, the displacement relationships between input and output for the improved architecture can be obtained from Equation (1) by replacing  $q_2$  with  $m \cdot \sin q_2$ , that is

$$\begin{cases} q_1 = \theta_1 \\ m \sin q_2 = e \sin \theta_2 \end{cases} \quad (5)$$

Let  $m = e$ , it follows that:

$$\left. \begin{aligned} q_1 &= \theta_1 \\ q_2 &= \theta_2 \end{aligned} \right\} \quad (6)$$

This implies that the direct linear one-to-one input-output correlation. Furthermore, it is interesting to note that Equations (2) and (4) still hold, but  $J$  becomes an identity matrix.

Since the new mechanism has the one-to-one input-output mapping, the kinematics is very simple. Both static and dynamic analyses can also be easily carried out. In addition, compared with the architecture in Figure 2, the new mechanism requires much smaller actuators.

#### 4 Workspace Analysis

As shown in Figure 5, the mechanism has two legs. The first leg ( $R_1$  to  $R_2$ ) produces the Euler angle  $\theta_1$  of the platform by the input of  $q_1$ ; while the second one ( $R_{10}$  to  $R_3$ ) produces  $\theta_2$  by  $q_2$ . To illustrate the motional relationship, let us introduce a transition parameter  $z$  to Equation (5), it follows that:

$$\left\{ \begin{aligned} q_1 &= \theta_1 \\ m \sin q_2 &= z = e \sin \theta_2 \end{aligned} \right. \quad (7)$$

where,  $z$  is the displacement of F-pair ( $R_4$  to  $R_6$ ) in the direction of  $z_1$ .

From Equation (7), it is seen that the Euler angle  $\theta_1$  is produced from the input of  $q_1$  directly by the first leg; while  $\theta_2$  is produced from  $q_2$  by the second leg through two transformations, which include (1) rotary to linear motion  $q_2 \Rightarrow z$  using  $m \cdot \sin q_2 = z$ , and (2) linear to rotary motion  $z \Rightarrow \theta_2$  using  $z = e \cdot \sin \theta_2$ . In the second transformation, there exists a limitation related to friction circle. Let  $\rho$  denote the radius of the friction circle of  $R_2$ , which is determined by the product of the radius  $r$  of the revolute joint's axis and the equivalent friction coefficient  $\mu$  as follows.

$$\rho = \mu r \quad (8)$$

Examining the force  $F$  of the F-pair acted onto the axis  $R_2$  of the moving platform (see Figure 6). Let  $\gamma$  denote the angle between  $z_1$  and the link  $\overline{R_2R_3}$ , and decompose the force  $F$  into two parts, the radial component  $F_r$  and the tangent component  $F_t$ . Then the force  $F$  acts on  $R_2$  is equivalent to a force  $Q$  and a torque  $M$ , which can be calculated from the following equations.

$$\left. \begin{aligned} Q &= F_r = F \cdot \cos \gamma \\ M &= F_t \cdot e = F \cdot e \cdot \sin \gamma \end{aligned} \right\} \quad (9)$$

As a basic law in mechanics, the effect of a

force  $Q$  and a torque  $M$  acting on a rigid body is equivalent to a force  $Q_h$  with an offset  $h$ , which is shown in figure 7 and can be calculated as follows

$$\left. \begin{aligned} Q_h &= Q \\ h &= M / Q = e \cdot \tan \gamma \end{aligned} \right\} \quad (10)$$

where,  $h$  is the distance between the action lines of force  $Q_h$  and  $Q$ .

There exist three instances for the different relationship between  $h$  and  $\rho$ , which are (1)  $h < \rho$ , the revolute joint  $R_2$  will never rotate regardless the value of  $Q_h$ ; (2)  $h > \rho$ , revolute joint  $R_2$  can rotate; and (3)  $h = \rho$ , the critical condition. In the critical condition of  $h = \rho$ , using Equation (10), it follows that:

$$\gamma = \arctan(\rho / e) \quad (11)$$

Then the work space of  $\theta_2$  satisfies:

$$-(\pi / 2 - \gamma) < \theta_2 < \pi / 2 - \gamma \quad (12)$$

On the other hand, the angle  $\theta_1$  produced by the first leg is limited only by the structure design of the F-pair and the base, so the workspace of  $\theta_1$  can reach a designated area through proper design. Assume that the workspace of  $\theta_1$  is from  $-\pi/2$  to  $\pi/2$ , then the workspace of the spherical mechanism can be depicted by the reachable range of the point  $P$  as shown in Figure 8.

When the mechanism is running, the direction of axis  $z_1$  keeps unchanged, while the direction of axis  $z_2$  alters according to  $\theta_1$ . So the workspace represented by spherical surface in Figure 8 can be interpreted as follows: point  $P$  draws latitude lines when only  $\theta_1$  changes and draws longitude lines while only  $\theta_2$  alters.

To simulate the potential actual workspace of the mechanism clearly, a prototype model is presented. Some Images of the prototype model in different configurations are introduced in figure 9.

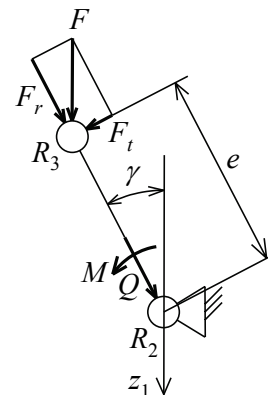


Fig. 6: Force and torque of  $R_2$

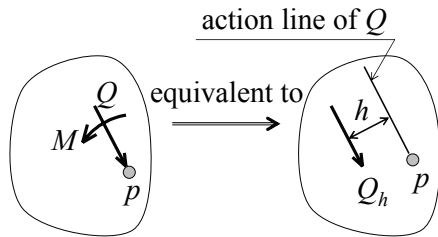


Fig.7: Force couple equivalent

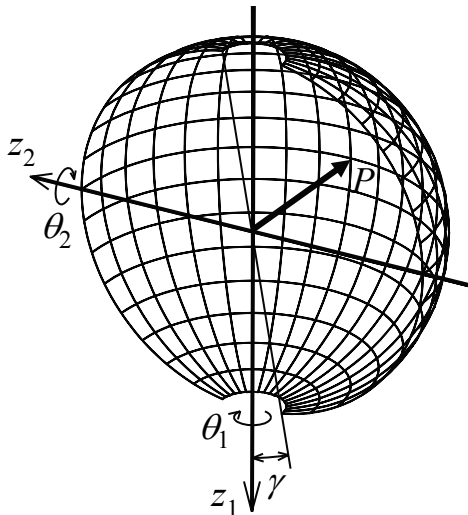


Fig. 8: The workspace of point P

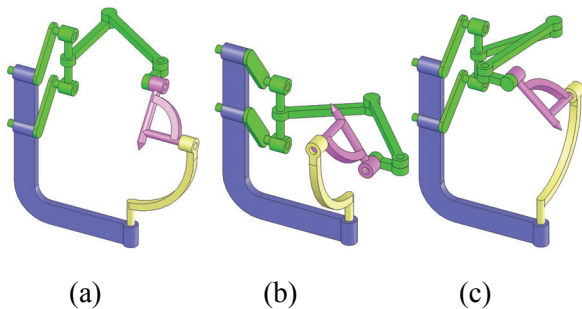


Fig. 9: Images of the prototype model in the configurations of (a)  $(\theta_1, \theta_2) = (0, \pi/3)$ , (b)  $(\theta_1, \theta_2) = (\pi/2, -\pi/4)$  and (c)  $(\theta_1, \theta_2) = (-\pi/2, \pi/4)$

## 5 Conclusions

In this paper, a parallel novel 2-DOF spherical mechanism with one-to-one input-output mapping is presented. This mechanism has a number of advantages including (a) the ability to position the payload at the geometric center of rotation thereby reducing inertia; (b) high stiffness enabling the use of high angular velocities and accelerations for orientating large payloads; (c) decoupled geometry making the forward and inverse kinematic calculation very simple; and (d) relatively large outward workspace (approximately a hemisphere)

and large internal free space for payload orientation. It is expected the new mechanism would find many applications.

### Acknowledgments:

The authors gratefully acknowledge the financial support of the National Natural Science Foundation of China (No. 50475055) and Hong Kong Innovation and Technology Commission (No. GHS/008/04).

### References:

- [1] V.E. Gough, S.G. Whitehall, "Universal Tyre Test Machine," *Proceedings of the 9<sup>th</sup> FISITA International Technical Congress*, pp. 117–137, May, 1962.
- [2] D. Stewart, "A Platform with Six Degrees of Freedom," *Proceedings of the Institution of Mechanical Engineers*, 180(15), 371–386, 1965, London, UK.
- [3] C.M. Gosselin, and J. Angeles, "The Optimum Kinematic Design of a Spherical Three-Degree-of-Freedom Parallel Manipulator," *Journal of Mechanisms, Transmissions, and Automation in Design*, 111(2), 202–207, 1989.
- [4] W.M. Craver and D. Tesar, "Force and Deflection Determination for a Parallel 3-DOF Robotic Shoulder Module," *1990 ASME Design Technical Conferences*, DE-Vol. 24, pp. 473–479, 1990, Chicago, IL.
- [5] C.M. Gosselin, and E. Lavoie, "On the Kinematic Design of Spherical Three-Degree-of-Freedom Parallel Manipulators," *International Journal of Robotics Research*, 12(4), 394–402, 1993.
- [6] S. Leguay-Durand and C. Reboulet, "Optimal Design of a Redundant Spherical Parallel Manipulator," *Robotica*, 15(4), 399–405, 1997.
- [7] C.W. Wampler, "Displacement Analysis of Spherical Mechanisms Having Three or Fewer Loops," *2002 ASME Design Engineering Technical Conferences*, Paper No. MECH-34326, 2002, Montreal, Canada.
- [8] R. Di Gregorio, "A New Parallel Wrist Using Only Revolute Pairs: the 3-RUU Wrist," *Robotica*, 19(3), 305–309, 2001.
- [9] R. Di Gregorio, "Kinematics of a New Spherical Parallel Manipulator with Three Equal Legs: the 3-URC Wrist," *Journal of Robotic Systems*, 18(5), 213–219, 2001.
- [10] M. Karouia, and J.M. Hervé, "A Family of Novel Orientational 3-DOF Parallel Robots," *The 14<sup>th</sup> CISM-IFTOMM Symposium*, pp.

- 359–368, 2002, Udine, Italy.
- [11] X. Kong, and C.M. Gosselin, “Type Synthesis of 3-DOF Spherical Parallel Manipulators Based on Screw Theory,” *2002 ASME Design Engineering Technical Conferences*, Paper No. MECH-34259, 2002, Montreal, Canada.
- [12] Z. Huang, and Q.C. Li, “Type Synthesis of Symmetrical Lower-Mobility Parallel Mechanisms Using Constraint Synthesis Method,” *International Journal of Robotics Research*, 22(1), 59–79, 2003.
- [13] P. Vischer, and R. Clavel, “Argos: a Novel 3-DOF Parallel Wrist Mechanism,” *International Journal of Robotics Research*, 19(1), 5-11, 2000.
- [14] V. Hayward, and R. Kurtz, “Modeling of a Parallel Wrist Mechanism with Actuator Redundancy,” *Advances in Robot Kinematics*, S. Stifter and J. Lenarčič, ed., pp. 444–456, Springer-Verlag, Wien, 1991.
- [15] C. Innocenti and V. Parenti-Castelli, “Echelon form Solution of Direct Kinematics for the General Fully Parallel Spherical Wrist,” *Mechanism and Machine Theory*, 28(4), 553–561, 1993.
- [16] K. Wohlhart, “Displacement Analysis of the General Spherical Stewart Platform,” *Mechanism and Machine Theory* 29(4), 581–589, 1994.
- [17] Y. Zhang, C. D. III Crane, and J. Duffy, “Determination of the Unique Orientation of Two Bodies Connected by a Ball-and-Socket Joint from Four Measured Displacements,” *Journal of Robotic Systems*, 15(5), 299–308, 1998.
- [18] M. Carricato, and V. Parenti-Castelli, “A Two-Decoupled-DOF Spherical Parallel Mechanism for Replication of Human Joints,” *Servicerob 2001 – European Workshop on Service and Humanoid Robots*, 2001, pp. 5–12, Santorini, Greece.
- [19] M. Carricato, and V. Parenti-Castelli, “A Novel Fully Decoupled Two -Degrees-of-Freedom Parallel Wrist,” *The International Journal of Robotics Research*, 23(6), 661-667, 2004.
- [20] L.W. Tsai, G.C. Walsh, and R. Stamper, “Kinematics of a Novel Three DOF Translational Platform,” *Proceedings of the 1996 IEEE International Conference on Robotics and Automation*, pp. 3446–3451, 1996, Minneapolis, MM.
- [21] L.W. Tsai, “Kinematics of a Three-DOF Platform Manipulator with Three Extensible Limbs,” *Recent Advances in Robot Kinematics*, J. Lenarčič, and V. Parenti-Castelli, ed., pp.401–410, Kluwer Academic Publishers, London, 1996.
- [22] T.S. Zhao and Z. Huang, “A Novel Three-DOF Translational Platform Mechanism and its Kinematics,” *2000 ASME Design Engineering Technical Conferences*, Paper No. MECH-14101, 2000, Baltimore, MD.
- [23] L. Baron and G. Bernier, “The Design of Parallel Manipulators of Star Topology under Isotropic Constraint,” *2001 ASME Design Engineering Technical Conferences*, Paper No. DAC-21025, 2001, Pittsburgh, PA.
- [24] J.M. Hervé, and F. Sparacino, “STAR: a New Concept in Robotics,” *International Conference of 3K-ARK*, pp. 176–183, 1992.
- [25] M. Carricato, V. Parenti-Castelli, A family of 3-DOF translational parallel manipulators, in: *Proceedings of the 2001 ASME Design Engineering Technical Conferences*, Pittsburgh, PA, DAC-21035, 2001.
- [26] X.W. Kong and C. Gosselin, “Kinematics and Singularity Analysis of a Novel Type of 3-CRR 3-DOF Translational Parallel Manipulator,” *International Journal of Robotic Research*, 21(9), 791–798, 2002.
- [27] H.S. Kim, and L.W. Tsai, “Design Optimization of a Cartesian Parallel manipulator,” *Journal of Mechanical Design*, 125(1), 43–51, 2003.
- [28] W.M. Li, F. Gao, and J.J. Zhang, “R-CUBE, a Decoupled Parallel Manipulator Only with Revolute Joints,” *Mechanism and Machine Theory*, 40(4), 467-473, 2005.
- [29] F. Gao, Y. Zhang, and W.M. Li, “Type Synthesis of 3-DOF Reducible Translational Mechanisms,” *Robotica*, 23(2) (2005) 239-245.